

Influence of interference on bearing capacity of strip footing on reinforced sand

M. Ghazavi & A.A. Lavasan

Civil Engineering Department, K.N. Toosi University of Technology, Tehran, Iran

ABSTRACT: Numerical evaluation of bearing capacity of interfered strip footing on unreinforced and reinforced sandy soils has been performed in this paper using finite difference method based on commercially available code, FLAC^{3D} (Fast Lagrangian Analysis of Continua). The failure criterion for the soil has been assumed to be based on Mohr-coulomb with non-associative flow rule by considering $0 \leq \psi < \varphi$. To ensure the accuracy of the constructed numerical models, the results obtained have been compared with available experimental and theoretical data. This comparison has validated the numerical modeling. Parametric studies have been carried out to determine the best locations for reinforcing layers in the forms of normalized ratios, for example width ratio, depth ratio, geogrid layer distance ratio, etc.). This facilitates to achieve the greatest values for bearing capacity of closely spaced strip footings. The results show that at low footing spacing, the bearing capacity increases sometimes up to three times compared with the case where no reinforcement is used. It has also found out that there is a certain spacing beyond which the bearing capacity decreases with increasing the distance between footings. With further increase in footing distance, the interference effect vanishes.

1 INTRODUCTION

Due to heavy loads exerted from superstructures to closely constructed shallow foundations on the ground surface. There is interference between footings. The interference between closely spaced footings may have effects on bearing capacity, settlement, and rotation of closely spaced footings.

Each of aforementioned conditions can affect design factors qualitatively. Some studies have been performed to investigate the bearing capacity of interfered footings on unreinforced soil (Stuart, 1962; Das & Larbi-Cherif, 1983 a, b; Graham et al., 1984; Kumar & Saran, 2003; Wang & Jao, 2002). With growing technology, significant promotion has been achieved in soil reinforcement. Thus, the subject of bearing capacity improvement has been of concern significantly. Different types of reinforcement have been used to reinforce soil beneath footings, for instance, metal strips (Binquet & Lee, 1975; Fraszgy & Lawton, 1984; Huang & Tatsuka, 1988), metal bars (Huang & Tatsuka, 1990), rope fibers (Akinmusuru & Akinboladeh, 1981), geotextiles (Guido et al., 1986), and geogrids (Guido et al., 1986; Yetimoglu et al., 1994; Omar et al., 1993a,b; Adams & Collin, 1997; Das & Shin, 1999). These studies have shown more encouragement in the use of geogrid to improve behaviors of spread footing mainly because of the stiffness of geogrid. Further research work has led to developing non-dimensional bearing capacity

ratio for soil reinforcement effects showing benefits of reinforcement. This non-dimensional ratio, BCR, is defined as

$$BCR = \frac{q_{u(R)}}{q_u} \quad (1)$$

where $q_{u(R)}$ is the ultimate bearing capacity with soil reinforcement and q_u is the ultimate bearing capacity without reinforcement.

Figure 1 shows two interfered shallow strip foundations of width B supported by a soil reinforced with layers of geogrid. Character N represents the number of geogrid layers. The width of each geogrid layer is denoted by b. Parameter u depicts the depth of the closest geogrid layer from footing. The vertical distance between consecutive layers of geogrid is shown by h. Center to center spacing between two interfered footings is illustrated with Δ .

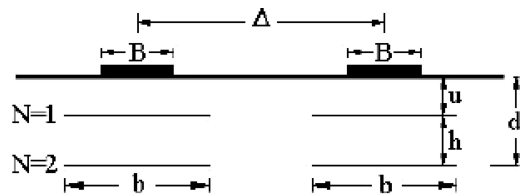


Figure 1. Geometry of two interfered strip footings supported by geogrid-reinforced soils.

To evaluate the bearing capacity of interfered footings on reinforced soil, the interference factor, I_f , may be defined as:

$$I_f = \frac{q_{uN(\text{interfered})}}{q_{u(\text{single})}} \quad (2)$$

where $q_{uN(\text{interfered})}$ is the ultimate bearing capacity of interfered footing with N layers of reinforcement and $q_{u(\text{single})}$ is the ultimate bearing capacity of same single footing with no reinforcement.

In recent years, some attempts have been devoted to the failure mechanism of reinforced soil (Huang & Tatsuka, 1988, 1990; Yamamoto & Otani, 2002; Michalowski & Shi, 2003). Two different mechanisms are offered. “Deep footing effect” which occurs in soil with short reinforcement and “width slab effect” associated with reinforcement extending considerably beyond the influenced zone by the footing.

The failure mechanism of interfered footings on both unreinforced and reinforced soil has not been considered comprehensively. Thus, this paper focuses on determining the bearing capacity of interfered strip footings on reinforced and unreinforced sand and also investigating the failure mechanism in different condition.

2 NUMERICAL ANALYSIS PROCEDURE

In the present numerical study, finite difference program FLAC^{3D} (Itasca Group, 2002) was used to model strip interfered footings constructed on unreinforced and reinforced sand. It uses an explicit, time marching method to solve the governing field equations. The Mohr-Coulomb failure criterion was used for prediction of soil behavior. Due to the symmetry of the soil-footing system and decrease the analysis time, only half part of the system was simulated. Rigid rough-base footings were assumed in parametric studies. It is assumed that the strip footing has a width of 1 m. To ensure the independency between bearing capacity and both boundary conditions and model dimension, the width and depth of soil-footing system was assumed to be 10B in both lateral and vertical directions, where B is the footing width. A maximum settlement of $s = 10\%B$ was applied to all models with a constant velocity of 5×10^{-7} m/step. Typical mesh of interfered model is shown in Figure 2.

2.1 Soil properties

Mechanical parameters of the soil, which were used in numerical modeling are presented in Table 1. The difference between ϕ and ψ represents a non associated plastic flow rule which means the plastic potential surface is not identical to the yield surface. Yin et al.

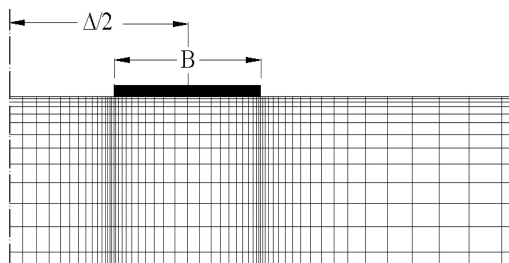


Figure 2. Typical mesh shape used in numerical FLAC model of interfered strip footing.

Table 1. Mechanical properties of soil and reinforcement.

Soil parameters		geogrid parameters	
Bulk modulus	2×10^4 kPa	Elasticity modulus	5.0×10^6 kPa
Shear modulus	1×10^4 kPa	Poisson ratio	0.3
cohesion	0.5 kPa	interface parameters	
friction	35°	Stiffness per unit area	2.39×10^6 kN/m ³
Dilation	20°	Cohesion	0
		friction	28°

(2001), Erickson & Drescher (2002), Frydman & Burd (1997) and De Borst & Vermeer (1984) found that the dilation angle has a significant influence on the numerical estimation of the footing bearing capacity. This dependence is more significant for higher values of the friction angle. According to previous study on determination of bearing capacity with FLAC, more accurate results can be obtained by considering dilation angle of soil about 2/3 friction angle. By using less dilation angle, local shear failure appears and by increasing dilation angle it tends to change to general shear failure. The difference between ϕ and ψ dictates the use of non-associated flow rule. Mechanical properties of soil are shown in Table 1.

2.2 Reinforcement properties

In FLAC^{3D}, the geogrid behaves as an isotropic linear elastic material with no failure limit. A shear directed (in the tangent plane to the geogrid surface) frictional interaction occurs between the geogrid and the soil grids, and the geogrid is slaved to the grid motion in the normal direction.

Because the settlement ratios were also small at failure for both unreinforced and reinforced sand in the analysis (i.e. $s/B < 5\%$ at failure), the strains developed in the geogrid reinforcement were likely to be very small, too. Therefore, a constant modulus of elasticity of $E = 5.0 \times 10^6$ kPa was used for numerical

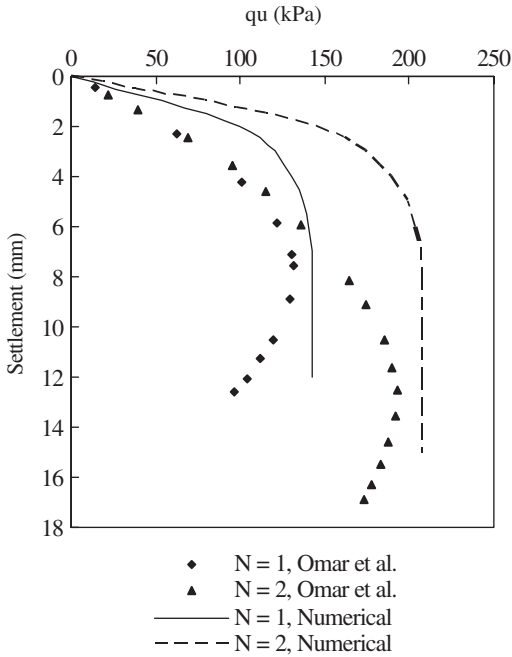


Figure 3. Results comparison of numerical and experimental methods.

analyses. To permit sliding between soil and geogrid, an interface element was used on both sides of reinforcement layers. The shear behavior of the geogrid-soil interface is cohesive and frictional in nature and is controlled by the coupling spring properties of: (1) stiffness per unit area; (2) cohesive strength; and (3) friction angle.

3 VERIFICATION OF NUMERICAL MODELING

To ensure the accuracy and capability of the numerical modeling, laboratory test of Omar et al. (1993 a, b) on bearing capacity of strip footing on reinforced silica sand with geogrid was simulated numerically and the results were compared. They used a $1.1 \times 0.914 \times 0.304$ m tank for their tests. The strip footing was 76.2×304 mm in plan.

The sand had an average dry unit weight of $\gamma_d = 17.14$ kN/m³ and a relative density of 70%. These were the same in all tests. The peak friction angle of the sand was 41°. A biaxial polypropylene polymer geogrid with nominal thickness of 1 mm was used for reinforcement. A comparison of numerical and experimental results is presented in Figure 3. As seen, a good agreement between numerical and experimental results exists and this indicates the capability of numerical modeling to predict the behavior of reinforced soil.

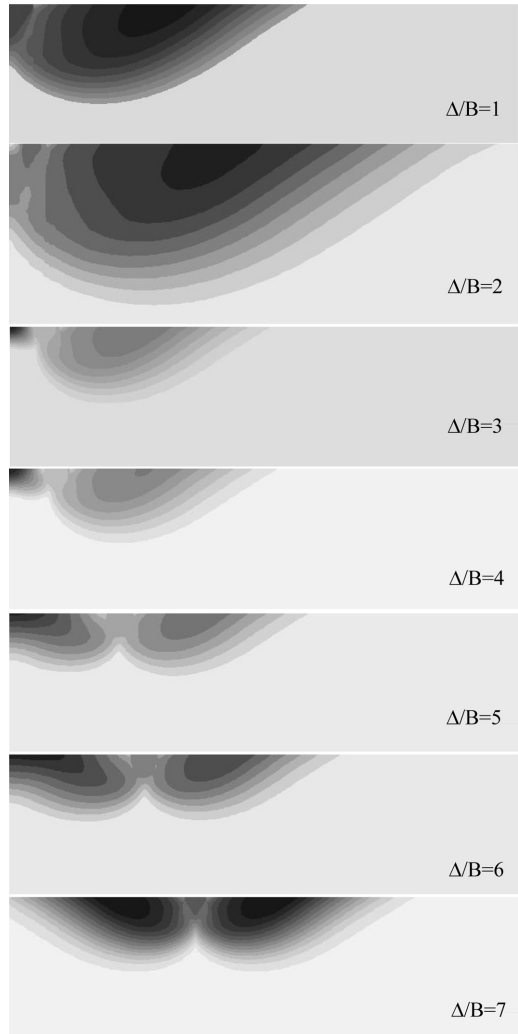


Figure 4. Displacement mechanism at different spaces.

4 ANALYSIS RESULTS AND DISCUSSIONS

4.1 Interfered strip footing on unreinforced sand

The first group of numerical analysis was conducted on unreinforced sand. Variations of displacement mechanism at different spacing for half of model were shown in Figure 4. As seen in Figure 4a, when $\Delta/B = 1.0$ (no distance exists between footings) system acts like a single foundation with a width equal to $2B$. The mechanism in Figure 4a coincides to that proposed by Prandtl (1920). At $\Delta/B = 2.0$ (Figure 4b), the “blocking” occurs and both footings act as a single foundation with width more than $2B$. An increase in the shape of spiral confirms this postulate. By increasing the distance between two neighboring

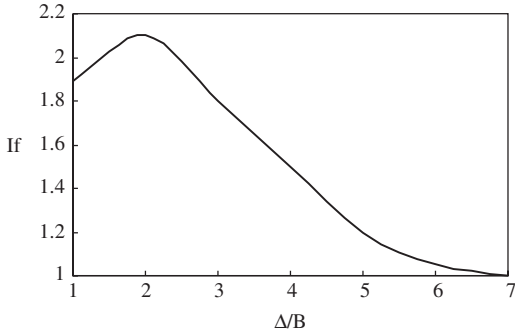


Figure 5. Variation of interference factor at different spacing on unreinforced sand.

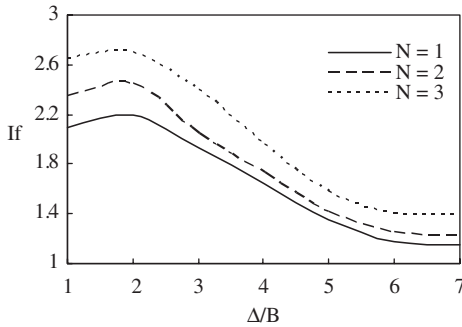


Figure 6. Variation of interference factor at different spacing on short width reinforced sand ($b/B = 1.5$; $u/B = h/B = 0.3$).

foundations, the influence of interference on footing behavior decreases.

The variation of the failure mechanism of unreinforced soil is in accordance with that proposed by Stuart (1962). A fluctuation of interference factor, I_f , at different spacings for interfered strip on unreinforced sand is exhibited in Figure 5. It is obvious from Figure 5 that by increasing Δ/B from 1 to 2, the bearing capacity increases. This is due to the blocking effect on failure mechanism as mentioned before. For Δ/B greater than 2, I_f value decreases gradually and interference effect on the bearing capacity disappears at $\Delta/B > 6$.

4.2 Interfered strip footing on reinforced sand with short layers of geogrid

The second numerical analysis group was conducted on reinforced sand with maximum 3 layer of short width geogrid ($b/B = 1.5$). These analyses were performed to evaluate the variation of bearing capacity with different number of reinforcement layers. For these tests, the parameters were $u/B = h/B = 0.3$; $b/B = 1.5$ and $N = 1, 2$ and 3.

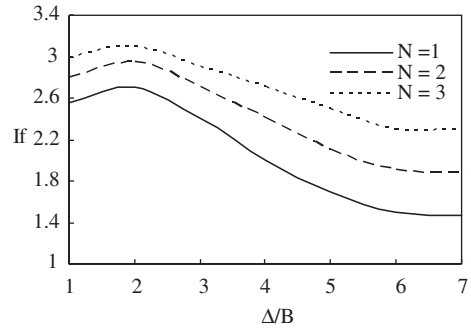


Figure 7. Variation of interference factor at different spacing on short width reinforced sand ($b/B = 5$; $u/B = h/B = 0.3$).

As shown in Figure 6, an increase in the number of reinforcement layers causes the interference factor to increase.

4.3 Interfered strip footing on reinforced sand with wide layers of geogrid

The last series of analysis was conducted to evaluate the effect of using wide layers of reinforcement layers on interference factor. These tests were performed on geometric parameters $u/B = h/B = 0.3$; $b/B = 1.5$ and $N = 1, 2$ and 3. The variation of I_f with space between closely spaced strip footings s shown in Figure 7. The difference between vertex quantity of curves and other parts decreases by using wide reinforcement layers.

5 DESIGN CHARTS

Based on preceding discussions, the variation of I_f at different spacings for three combination of soil reinforcing $N = 0, 1, 2$ and 3, design charts of interfered strip footings on unreinforced and reinforced sand are presented. For practical design purposes, the distance between closely spaced footings is normally determined by architectural restriction. In the subsequent section, the first step is to determine the number of reinforcing geogrid for the expected bearing capacity. Therefore, in this charts, variations of interference factor at each spacing ratio for any number of reinforcement between 0 to 3 are illustrated. By the use of these charts, the width and number of reinforcement layers could be determined to receive required bearing capacity (Figures 8–9).

6 CONCLUSIONS

The results of a number of numerical analyses on surface rough strip foundation on unreinforced and

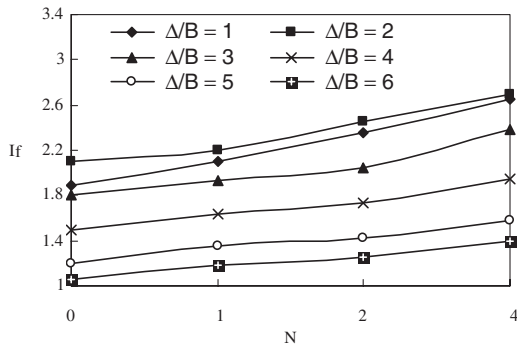


Figure 8. Variation of interference factor with respect to number of reinforcement at different footing spacings.

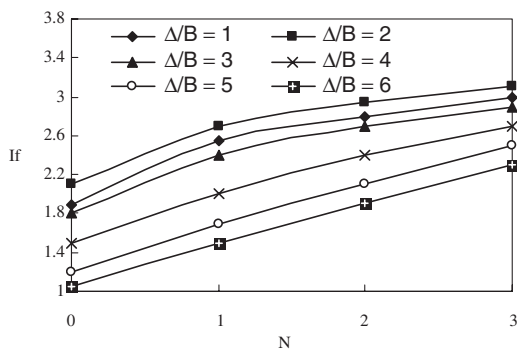


Figure 9. Variation of interference factor at different spacing.

reinforced sand were presented. Based on these analyses, following general conclusions can be pointed out:

1. When two neighboring footings are constructed besides (no distance exists between 2 footings), both footings act like a single footing with $2B$ width in both unreinforced and reinforced sand.
2. The bearing capacity of interfered strip footing is maximized at $\Delta/B = 2$ for reinforced and unreinforced sand.
3. The influence of interference disappears at footing spacing more than about $6B$.
4. Using wide layers of reinforcement leads to greater bearing capacity.

REFERENCES

Adams, M.T. & Collin, J.G. 1997. Large Model Spread Footing Load Tests on Geosynthetic Reinforced Soil Foundations. *Journal of Geotechnical and Geoenvironmental Engineering*, ASCE, Vol. 123, No. 1, pp. 66–72.

Akinmusuru, J.O. & Akinboladeh, J.A. 1981. Stability of Loaded Footings on Reinforced Soil. *Journal of Geotechnical and Geoenvironmental Engineering*, ASCE, Vol. 107, No. 6, pp. 819–827.

Binquet, J. & Lee, K.L. 1975. Bearing Capacity Tests on Reinforced Earth Slabs. *Journal of Geotechnical and Geoenvironmental Engineering*, ASCE, Vol. 101, No. 12, pp. 1241–1255.

Das, B.M. & Larbi-Cherif, S. 1983a. Bearing Capacity of Two Closely Spaced Shallow Foundations on Sand. *Soils and Foundations*, Vol. 23, No. 1, pp. 1–7.

Das, B.M. & Larbi-Cherif, S. 1983b. Ultimate Bearing Capacity of Closely Spaced Strip Foundations. *TRB, Transportation Research Record*, Vol. 945, pp. 37–39.

Das, B.M. & Shin, E.C. 1999. Bearing Capacity of Strip Footing on Geogrid-Reinforced Sand. *11th Asian Regional Conference on Soil Mechanics and Geotechnical Engineering*, Hong, Rotterdam, pp. 189–192.

De Borst, R. & Vermeer, P.A. 1984. Possibilities and Limitations of Finite Elements for Limit Analysis. *Geotechnique*, Vol. 34, No. 2, pp. 199–210.

Erickson, H.L. & Drescher, A. 2002. Bearing Capacity of Circular Footings. *Journal of Geotechnical and Geoenvironmental Engineering*, ASCE, Vol. 128, No. 1, pp. 38–43.

Fragaszy, R.J. & Lawton, E.C. 1984. Bearing Capacity of Reinforced Sand Subgrades. *Journal of Geotechnical and Geoenvironmental Engineering*, ASCE, Vol. 110, No. 10, pp. 1500–1507.

FLAC-Fast Lagrangian Analysis of Continua, 2002, Version 2.1., *ITASCA Consulting Group, Inc.*, Minneapolis.

Graham, J. & Raymond, G.P. & Suppiah, A. 1984. Bearing Capacity of Two Closely Spaced Footings on Sand. *Geotechnique*, Vol. 34, No. 2, pp. 173–182.

Guido, V.A. & Chang, D.K. & Sweeney, M.A. 1986. Comparison of Geogrid and Geotextile Reinforced Earth Slabs. *Canadian Geotechnical Journal*, Vol. 23, pp. 435–440.

Huang, C.C. & Tatsuoka, F. 1988. Prediction of Bearing Capacity in Level Sandy Ground Reinforced With Strip Reinforcement. *Proceedings of International Geotechnical Symposium on Theory and Practice of Earth Reinforcement*, Fukuoka, Kyushu, Japan, pp. 191–196.

Huang, C.C. & Tatsuoka, F., 1990. Bearing Capacity of Reinforced Horizontal Sandy Ground. *Geotextiles and Geomembrans*, Vol. 9, No. 1, pp. 51–82.

Kumar, A. & Saran, S. 2003. Closely Spaced Footings on Geogrid-Reinforced Sand. *Journal of Geotechnical and Geoenvironmental Engineering*, ASCE, Vol. 129, No. 7, pp. 660–664.

Michalowski, R.L. & Shi, L. 2003. Deformation Patterns of Reinforced Foundation Sand at Failure. *Journal of Geotechnical and Geoenvironmental Engineering*, ASCE, Vol. 129, No. 6, pp. 439–449.

Omar, M.T., Das, B.M., Yen, S.C., Puri, V.K. & Cook, E.E. 1993a. Ultimate Bearing Capacity of Rectangular Foundations on Geogrid-Reinforced Sand. *Geotechnical Testing Journal*, ASTM, Vol. 16, No. 2, pp. 246–252.

Omar, M.T., Das, B.M., Puri, V.K., Yen, S.C. 1993b. Ultimate Bearing Capacity of Shallow Foundations on Sand with Geogrid Reinforcement. *Canadian Geotechnical Journal*, Vol. 30, pp. 545–549.

Prandtl, L. 1920. Über die Härte plastischer Körper. *Nachr. Königl. Ges. Wissensch., Göttingen; Mathematisch physikalische Klasse*, pp. 74–85.

- Stuart, J.G. 1962. Interference Between Foundations with Special Reference to Surface Footings in Sand. *Geotechnique*, Vol 12, No. 1, pp. 15–23.
- Wang, M.C. & Jao, M. 2002. Behavior of Interacting Parallel Strip Footing. *Electronic Journal of Geotechnical Engineering*, Vol 7, part A.
- Yetimoglu, T., Wu, J.T.H. & Saglamer, A. 1994. Bearing Capacity of Rectangular Footings on Geogrid Reinforced Sand. *Journal of Geotechnical and Geoenvironmental Engineering*, ASCE, Vol. 120, No. 12, pp. 2083–2099.
- Yamamoto, K. & Otani, J. 2002. Bearing Capacity and Failure Mechanism of Reinforced Foundations Based on Rigid-Plastic Finite Element Formulation. *Geotextiles and Geomembrans*, Vol. 20, No. 1, pp. 367–393.
- Yin, J.H. & Wang, Y.J. & Selvadurai, A.P.S. 2001. Influence of Nonassociativity on the Bearing Capacity of a Strip Footing. *Journal of Geotechnical and Geoenvironmental Engineering*, ASCE, Vol. 127, No. 11, pp. 985–989.